Available online at www.sciencedirect.com
ScienceDirect
Journal of Molecular Catalysis A: Chemical 284 (2008) 127–133
JOURNAL OF MOLECULAR CATALYSIS A: CHEMICAL
www.elsevier.com/locate/molcata

# Degradation of $C_2H_2$ with modified-$TiO_2$ photocatalysts under visible light irradiation

Taizo Sano [a,b,*], Eric Puzenat [b], Chantal Guillard [b], Christaphe Geantet [b], Sadao Matsuzawa [a]

[a] *Institute for Environmental Management Technology, National Institute of Advanced Industrial Science and Technology (AIST), AIST Tsukuba West, 16-1 Onogawa, Tsukuba, Ibaraki 305-8569, Japan*

[b] *Institut de recherches sur la catalyse et l'environnement de Lyon (IRCELYON), Université Claude Bernard Lyon1, Bât J. Raulin, 43 bd du 11 Novembre 1918, 69622 Villeurbanne Cedex, France*

Received 22 September 2007; received in revised form 29 December 2007; accepted 10 January 2008
Available online 18 January 2008

**Abstract**

Photocatalytic degradation of $C_2H_2$ by nitrogen-doped $TiO_2$ (N-$TiO_2$), nitrogen and carbon-doped $TiO_2$ (NC-$TiO_2$), BA-PW25 (commercialized as oxygen deficient $TiO_2$ ($TiO_{2-\delta}$) photocatalyst), and P25 (conventional $TiO_2$) were analyzed. Only BA-PW25 photocatalyst decomposed $C_2H_2$ into $CO_2$ under visible light ($\lambda > 400$ nm), while the other photocatalysts did not change $C_2H_2$. From the analyses of the byproduct formation and the reaction rate of $C_2H_2$ degradation, it is inferred that the active species effective for $C_2H_2$ degradation were formed on the mid-gap level of BA-PW25 at the potentials between the valence-band top of conventional $TiO_2$ and the N-induced mid-gap level of N-$TiO_2$.


*Keywords:* Visible light; Oxygen-deficient $TiO_2$; Photocatalytic degradation; Acetylene; Nitrogen doping

## 1. Introduction

Titanium dioxide ($TiO_2$) shows photocatalytic activity for oxidative removals of environmental pollutants, such as $NO_x$ and VOC, under ultraviolet irradiation ($\lambda < 380$ nm) [1–3]. However, since pure $TiO_2$ acts as photocatalyst with ultraviolet (UV) light, the efficiency of $TiO_2$ in a closed environment, where UV light is insufficient, is generally low. The $TiO_2$ photocatalyst can be utilized more beneficially if it is activated with visible-light.

Recently, the doping of anion, such as N, C, S, and F, into $TiO_2$ has been recognized to provide the visible-light responsibility [4–13]. Nitrogen-doped $TiO_2$ (N-$TiO_2$) was prepared by reduction with gaseous $NH_3$, hydrolysis of titanium salt by ammonia solution, or sputtering. N-$TiO_2$ oxidized acetaldehyde, 2-propanol and CO into $CO_2$ in dry air with visible light [5–7], while N-$TiO_2$ did not oxidize $HCOO^-$ in aqueous phase [8]. Sano et al. [9] succeeded in the preparation of different type of N-doped $TiO_2$ from titanium–bipyridine complex. The newly prepared $TiO_2$ oxidized NO under visible light with longer wavelengths ($\lambda < 650$ nm), however, it did not degrade acetaldehyde. The presence of carbon atom in the anatase lattice could explain the different activities from the conventional N-$TiO_2$. Although the presence of lattice carbon has not been confirmed completely, the photocatalyst prepared from titanium–bipyridine complex is denoted in this paper as nitrogen and carbon doped $TiO_2$ (NC-$TiO_2$) for convenience.

Doping of oxygen defect is another method to produce visible-light responsible $TiO_2$. The $H_2$-plasma treatment of ultrafine particle of $TiO_2$ caused the creation of oxygen defects in anatase lattice, and the formed oxygen-deficient $TiO_2$ ($TiO_{2-\delta}$) oxidized NO under visible light up to ca. 600 nm [14]. Ihara et al. [15] reported the synthesis of oxygen-deficient $TiO_2$ in aqueous phase. They concluded that the oxygen-deficient sites formed at grain boundaries of $TiO_2$ polycrystallite were important to emerge visible-light responsibility and that the nitrogen atom doped in part of oxygen defects worked as a blocker for reoxidation. BA-PW25 (Ecodevice Co.) is a pale-yellow powder prepared by the calcination of titanium

* Corresponding author at: Institute for Environmental Management Technology, National Institute of Advanced Industrial Science and Technology (AIST), AIST Tsukuba West, 16-1 Onogawa, Tsukuba, Ibaraki 305-8569, Japan. Tel.: +81 29 861 8451; fax: +81 29 861 8866.
*E-mail address:* sano-t@aist.go.jp (T. Sano).

1381-1169/$ – see front matter © 2008 Published by Elsevier B.V.
doi:10.1016/j.molcata.2008.01.014

hydroxide precursor made from titanium (IV) sulfate and ammonia solution [16]. This preparation method is similar to that described by Ihara et al. [15]. BA-PW25 is one of the photocatalysts commercialized as visible-light responsible $TiO_2$, and its visible light responsibility is attributed to the oxygen-deficiency of $TiO_2$ by the company. BA-PW25 photocatalyst degraded 2-propanol and acetone into $CO_2$ under blue LED light ($\lambda \approx 430$ nm). In a preliminary analysis with X-ray photoelectron spectroscopy (XPS), N atom was not observed in BA-PW25, although ammonia solution was used in the preparation process.

The basic knowledge on the purification of air and water by visible-light responsive $TiO_2$ is quite primitive, in contrast with that on conventional $TiO_2$ which is well studied. It is not clear what kinds of chemical substances can be mineralized or not by visible-light responsive photocatalyst. The utilization of visible light by modified-$TiO_2$ is strongly related to the modification of the band structure, which may decrease the oxidative power for pollution substances. The degradation of acetaldehyde, 2-propanol, and NO in dry air has been already reported [5,6,9,11,12,14], however, there are few reports that investigate the degradation of other organic compound in gaseous phase. The degradation of $C_2H_2$ is an interesting subject to be studied with visible-light responsive photocatalyst, since the oxidation of $C_2H_2$ is much more difficult than that of acetaldehyde; the reaction rate constants of OH radical with either $C_2H_2$ or acetaldehyde are 78 or 1600 ($10^{-14}$ cm$^3$ molecule$^{-1}$ s$^{-1}$), respectively [17,18].

In the present study, we analyzed the degradation of $C_2H_2$ by N-$TiO_2$, NC-$TiO_2$, BA-PW25 (as $TiO_{2-\delta}$) and P25 photocatalysts under visible light, and evaluated their oxidative powers. Especially, the $C_2H_2$ degradation by BA-PW25 was analyzed in detail since it showed the highest degradation rate of $C_2H_2$. The byproduct formation, the reaction rate constant, and the absorption constant were compared with those of conventional $TiO_2$.

## 2. Experimental

### 2.1. Preparation of photocatalysts

N-$TiO_2$ was prepared by $NH_3$ treatment of anatase type $TiO_2$ using ST-01 (Ishihara sangyo Co.). The ST-01 powder (3.0 g) was placed in a single path reactor of quartz, then heated to 600 °C and hold at this temperature for 3 h in a $NH_3$/Ar (10%) carrier gas. NC-$TiO_2$ was prepared by calcination of $Ti^{4+}$–bipyridine complex precursor at 300 °C, followed by isothermal holding in Ar gas stream at 380 °C for 12 h [9]. BA-PW25 (Ecodevice Co.) and P25 (Degussa) were used without any prior treatment. The solid phases were identified by X-ray diffractometry (XRD) with Cu Kα radiation (Rigaku, Model RU-300), UV–vis diffuse reflectance spectroscopy (PerkinElmer, Lambda 45), and thermo gravimetry with differential thermal analysis (TG-DTA) (SETARAM, Setsys Evolution 1200).

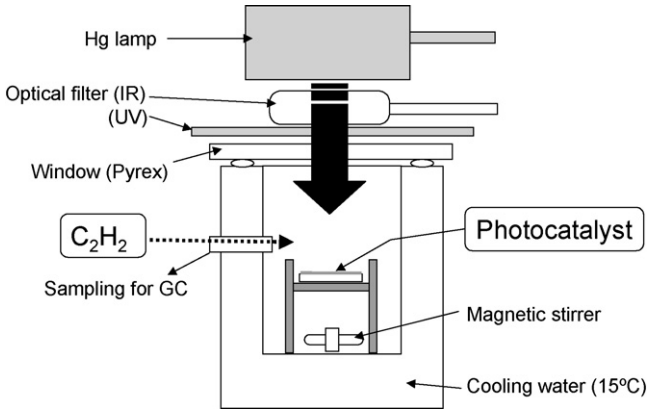


Fig. 1. Illustration of batch-type photocatalytic reactor.

### 2.2. Photocatalytic degradation of $C_2H_2$

A suspension of 40 mg photocatalyst powder in 1 ml distilled water was dispersed on a glass plate (9.0 cm$^2$), then dried at 110 °C for 1 day. The photocatalyst was weakly bound on the glass plate and was physically stable during experiments. The glass with photocatalyst was placed in a batch reactor (320 cm$^3$) with a cover window of Pyrex glass (Fig. 1). The temperature of the reactor was maintained at 15 °C by cooling water. A light source (Philips HPK-125 W) was placed on the upper side of the reactor. A water cell was placed between the reactor and the light source to absorb infrared light. The light passed thorough the water cell contained both of UV light photons and visible light photons. In this paper, the irradiation of these photons is simply denoted as "UV irradiation" since the effect of UV light is normally dominant. In the typical experimental condition, the "UV irradiation" was composed of a UV photon flux of $4.7 \times 10^{-9}$ mol cm$^{-2}$ s$^{-1}$ ($300 < \lambda < 380$ nm) and a visible-light photon flux of $2.9 \times 10^{-9}$ mol cm$^{-2}$ s$^{-1}$ ($380 < \lambda < 600$ nm) at the sample surface. In the photocatalytic reaction with only visible light, a UV-cut filter (Sumitomo kagaku, LF-41) was placed between the water cell and the reactor, and the distance between the sample and the light source was shortened with respect to that used with UV irradiation. The transmittance of LF-41 were 0.05%, 1% and 90%, at 380 nm, 400 nm and wavelengths longer than 430 nm, respectively. The photon flux in visible-light region was $3.1 \times 10^{-8}$ mol cm$^{-2}$ s$^{-1}$ ($380 < \lambda < 600$ nm). The UV intensity was less than the detection limit (1 μW cm$^{-2}$) of UV analyzer (Vilber Lourmat, VLX-3W with CX-365). The reactor was filled with synthetic air, and then with the required amount of $C_2H_2$ gas (Air Liquide) was introduced. Visible or UV light was irradiated to the photocatalyst while the reaction atmosphere was vigorously stirred by a magnetic stirrer. The concentrations of $C_2H_2$ and $CO_2$ were analyzed by gas chromatography with Flame Ionization Detector (Intersmat; FID IGC120 FL) and Thermal Conductivity Detector (TCD).

Acidic byproducts formed on the photocatalyst powder were analyzed with high-performance precision liquid chromatography (HPLC, Varian Inc., ProStar HPLC system equipped with Sarsep Car-H column). The photocatalyst used for $C_2H_2$ degradation was dispersed into 2.0 ml of $H_2SO_4$ solution

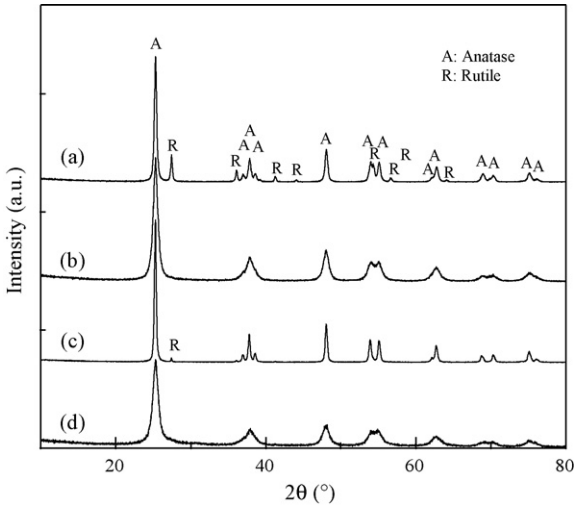


Fig. 2. XRD spectra of (a) $TiO_2$ (P25), (b) BA-PW25, (c) N-$TiO_2$ and (d) NC-$TiO_2$.

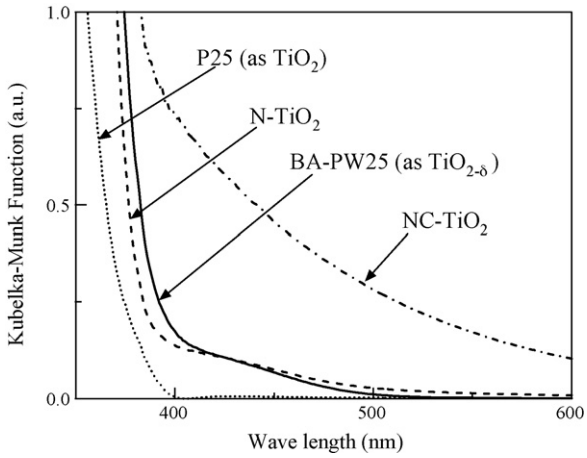


Fig. 3. UV–vis spectra of visible-light responsive photocatalysts measured by diffuse reflectance method.

$(6 \times 10^{-3}\ \mathrm{mol\,dm^{-3}})$ and then subjected to ultrasonication for 10 min. After the elution for 1 day, the eluate was analyzed by HPLC.

## 3. Results and discussion

### 3.1. Characterization of photocatalysts

Fig. 2 shows the XRD spectra of P25, BA-PW25, N-$TiO_2$, and NC-$TiO_2$. In each photocatalyst the anatase phase was dominant, whereas P25 and N-$TiO_2$ contained a small amount of rutile phase. The major peaks of BA-PW25 and NC-$TiO_2$ were broader than that of P25 and N-$TiO_2$, indicating that the powders consisted of ultrafine crystallites. The crystallite size of BA-PW25 was estimated to be 20 nm by Sherrer's equation. The structure parameters of BA-PW25 were refined by the Rietveld method from the X-ray diffraction data with RIETAN-2000 [19]. The spectrum was well fitted to the single phase of anatase; the goodness-of-fit indicator, $S$, was 1.05. The lattice parameters $a_o$ and $c_o$ were $0.381 \pm 0.007$ nm and $0.96 \pm 0.02$ nm, respectively, not so significantly different from those of the conventional $TiO_2$. The occupation factor for $O^{2-}$ was $1.04 \pm 0.01$. For the other photocatalyst samples, the occupation factor for $O^{2-}$ was $1.01 \pm 0.01$. This suggests the bulk of BA-PW25 was not oxygen-deficient but cation-deficient.

In the UV–vis spectra of N-$TiO_2$ (Fig. 3), the absorption edge located at the longer wavelength (~395 nm) in comparison with the absorption edge of conventional $TiO_2$ (P25), and an absorption shoulder was observed in the visible region between 400 and 600 nm. This visible-light absorption was attributed to N ions doped in the anatase lattice [5–7,20,21], although the state of N has not been clarified yet. In the spectrum of BA-PW25, the red shift of absorption edge and the visible light absorption were observed. The absorption edge of BA-PW25 located at a slightly longer wavelength (400 nm) than that of N-$TiO_2$, and the absorption disappeared at 500 nm. Therefore, the electron structure related to the visible light absorption of BA-PW25 seems to be slightly different from that of N-$TiO_2$. Based on a density-functional theory (DFT) calculations [22], doping of oxygen defect in the anatase lattice formed donor states located below the conduction band edge of bare $TiO_2$ and induced the optical absorption in the visible-light region mainly above 500 nm. In addition, the absorption coefficient increased with wavelength up to 700 nm. Since the spectrum of BA-PW25 showed no absorption above 500 nm, BA-PW25 may not contain the kind of oxygen defect treated in the DFT calculation. For the UV–vis spectrum of NC-$TiO_2$, the obvious absorption edge was not observed and the protracted absorption continued above 800 nm. The wide-range absorption by NC-$TiO_2$ is explicable by assuming simultaneous incorporation of N and C into the anatase lattice [9].

We attempted to analyze the oxygen deficiency ($\delta$ in $TiO_{2-\delta}$) of BA-PW25 with TG-DTA (Fig. 4). Between the room temperature and 180 °C, a rapid weight loss of BA-PW25 with endothermic process was observed. Weight losses were also observed above 180 °C. These weight losses are ascribable to the release of adsorbed water. Neither significant exothermic peak nor weight increase was observed up to 800 °C. If the

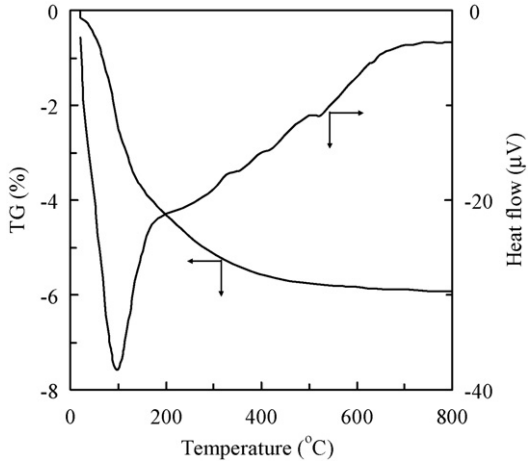


Fig. 4. Thermogravimetry with differential thermal analysis (TG-DTA) on BA-PW25 recorded in air stream at a heating rate of 5 K $min^{-1}$.

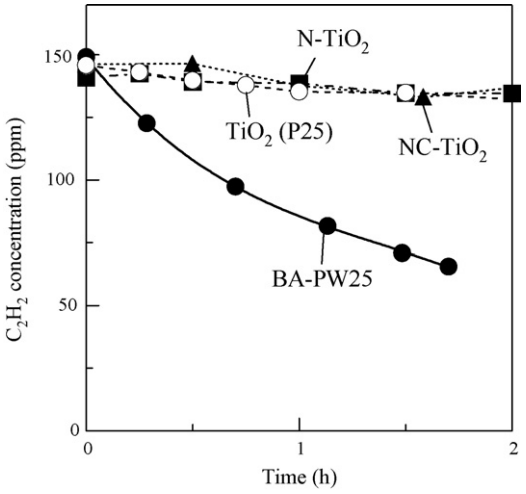


Fig. 5. Photocatalytic degradation of $C_2H_2$ under visible light irradiation.

bulk of BA-PW25 possessed an oxygen defect structure, incorporation of oxygen by oxygen defects could take place at the measured temperature range, thus resulting in a weight increase and in an exothermic peak. It is suggested that the bulk of BA-PW25 is nearly stoichiometric and that the oxygen deficiency $\delta$ is quite small (<0.01) even if oxygen defects are present. If oxygen-defects existed only around the surface or at the grain boundaries, as described by Ihara et al. [15], the detection by TG-DTA or XRD would be quite difficult. At this stage, we cannot find out any clear positive evidence for oxygen defect in BA-PW25.

### 3.2. Degradation of $C_2H_2$ by visible light responsive $TiO_2$

Fig. 5 shows the time courses of $C_2H_2$ concentrations with the photocatalysts under visible light. The change in the concentration was negligible for $TiO_2$ (P25), N-$TiO_2$, and NC-$TiO_2$. Only BA-PW25 decreased the $C_2H_2$ concentration. These results suggest that BA-PW25 successfully degrade $C_2H_2$ under visible light in contrast with the other photocatalysts which do not transform $C_2H_2$ in the present experimental conditions.

The photocatalytic degradation of $C_2H_2$ by BA-PW25 was further analyzed. To improve the accuracy of the mass balance, the initial concentration of $C_2H_2$ was set to the higher concentration (1000 ppm), and the formation of $CO_2$ was analyzed by gas chromatography (Fig. 6(a)). When the photocatalyst was irradiated with the visible light, the $C_2H_2$ concentration decreased rapidly from 1000 ppm to 100 ppm during the initial 50 h, and then decreased slowly. Concurrently, the $CO_2$ concentration increased rapidly to 1500 ppm for 50 h, and then increased quite slowly after 50 h. The slow reaction rates after 50 h may be due to the photocatalyst, impairment caused by the adsorbed water [8] or the byproduct formation. In the ideal mineralization of $C_2H_2$, one $C_2H_2$ molecule decomposed into two $CO_2$ molecules as Eq. (1).

$$C_2H_2 + \frac{5}{2}O_2 \rightarrow 2CO_2 + H_2O \quad (1)$$

However, the amount of $CO_2$ formed was smaller than twice of the amount of decreased $C_2H_2$. This suggests that the $C_2H_2$ removed from the gas phase was not completely decomposed into $CO_2$. Since neither CO nor an organic compound, except for $C_2H_2$, was detected in the gas phase, some byproducts-containing carbon must be adsorbed on the photocatalyst. The total amount of byproducts was estimated from the mass balance of $C_2H_2$ and $CO_2$, and was plotted as gaseous $C_1$ compound.

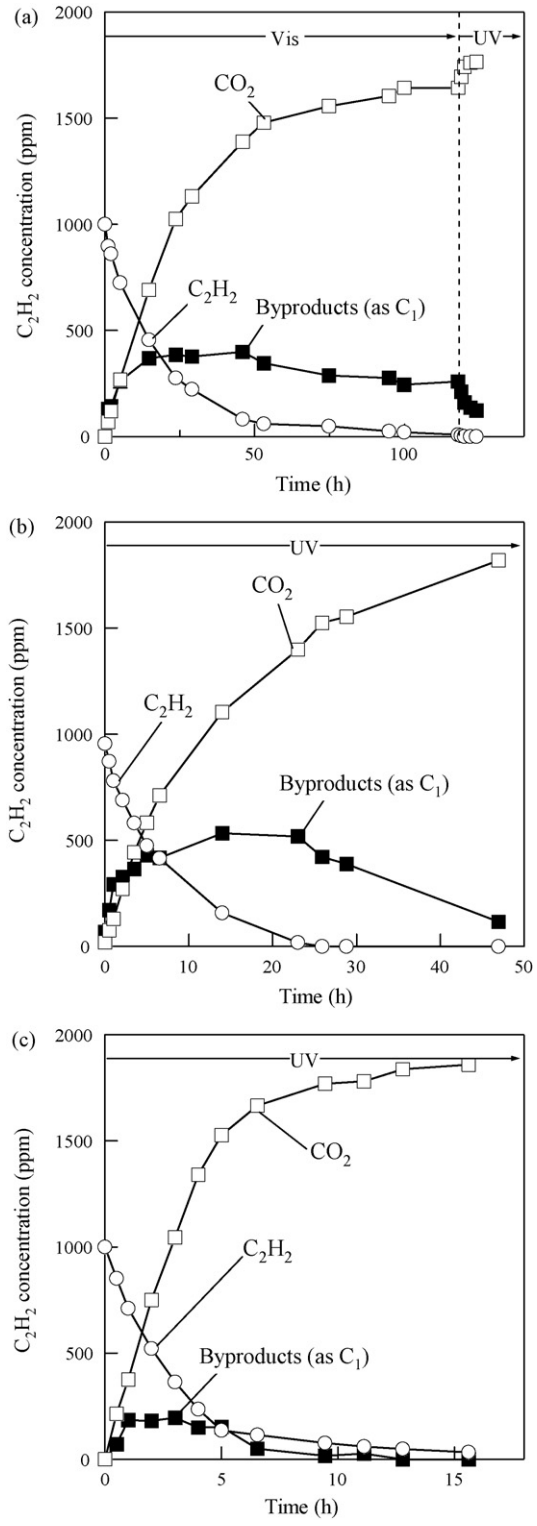


Fig. 6. $C_2H_2$ degradation profiles with (a) BA-PW25 under visible light, (b) BA-PW25 under UV light and (c) P25 under UV light.

The amount of byproducts increased in the initial stage (0–12 h), and then gradually decreased.

Acidic byproducts formed on the BA-PW25 powder were analyzed with HPLC. From the BA-PW25 powder, that had contacted with 1000 ppm of $C_2H_2$ for 5 h under visible light, 0.45 μmol (30 ppm as gaseous compound) of formic acid was detected. This amount corresponds to 13% of removed $C_2H_2$ molecules, which is high enough to be considered as an important intermediate. The amounts of acetic acid and oxalic acid were negligible, although these acids were detected as byproduct in the degradation of $C_2H_2$ by non-thermal plasma [23]. Also, aldehydes may not be byproducts in this system since the photocatalytic degradation of aldehydes were generally easier than that of formic acid. The powder after irradiation for 24 h contained only 0.03 μmol (2 ppm) of formic acid. This corresponds to 0.3% of the removed $C_2H_2$ and to 0.5% of the estimated byproduct. These results indicate that formic acid was formed on BA-PW25 in the initial stage of $C_2H_2$ degradation and that the formed formic acid was gradually transformed.

After the visible-light irradiation for 100 h, the formation of $CO_2$ became negligible, although the byproduct was remained in the reactor (Fig. 6(a)). To confirm the presence of organic byproduct on the photocatalyst, the UV-cut filter was removed and UV light was irradiated to the photocatalyst. As a result, 124 ppm of $CO_2$ formed by UV irradiation for 3 h, and then the $CO_2$ formation seemed to have completed. These results indicate that the BA-PW25 forms organic byproduct on its surface by visible light irradiation ($\lambda > 400$ nm) and that the formed byproduct is degradable to $CO_2$ by UV irradiation. It is inferred that the byproduct was a kind of polymer, which was hardly oxidized into $CO_2$ with visible light. The final concentration of $CO_2$ was not completely twice of the initial concentration of $C_2H_2$. This is due to the gas sampling of the reaction atmosphere for gas chromatography.

The formation of byproduct was temporally observed under UV light on BA-PW25 and P25 (Fig. 6(b) and (c)). The initial rate of decrease in the $C_2H_2$ concentration by BA-PW25 with UV was approximately twice of that with visible light. However the initial rate of $CO_2$-formation was significantly smaller than twice. As a result, the amount of byproduct temporally formed under UV light was larger than that under visible light. It seems that the BA-PW25 photocatalyst degraded preferentially $C_2H_2$ rather than the byproduct. After the $C_2H_2$ concentration became nearly zero (26 h), the byproduct was smoothly decomposed into $CO_2$. In the degradation by P25 under UV light, the amount of byproduct was significantly smaller than that by BA-PW25. The conversions of both $C_2H_2$ and $CO_2$ after an irradiation time, $t$, were defined as Eqs. (2) and (3), respectively, and plotted in Fig. 7.

$$C_2H_2\text{conversion}(\%) = ([C_2H_2]_0 - [C_2H_2]_t)/[C_2H_2]_0 \times 100 \quad (2)$$

$$CO_2\text{conversion}(\%) = [CO_2]_t/2[C_2H_2]_0 \times 100 \quad (3)$$

If all the $C_2H_2$ removed from the gas phase were oxidized into $CO_2$, the $CO_2$ conversion would be equal to the $C_2H_2$ conversion

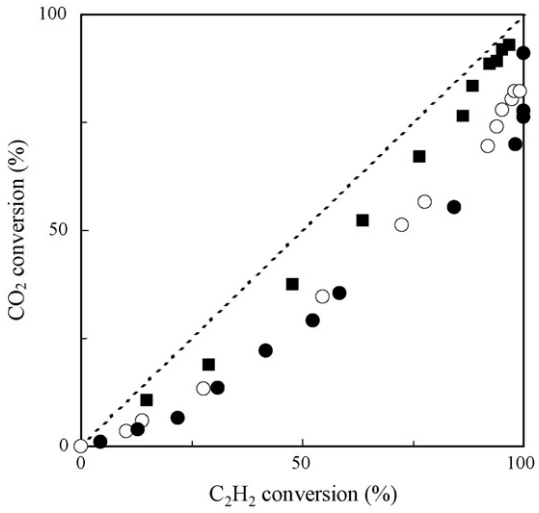


Fig. 7. $CO_2$ conversion as a function of $C_2H_2$ conversion defined as Eqs. (2) and (3). (◯) BA-PW25 under visible light, (●) BA-PW25 under UV light and (■) P25 under UV light.

(broken line). The vertical distance from the broken line to the plot is proportional to the amount of byproduct. The amount of byproduct formed by P25 under UV-light was smallest, and the amount formed by BA-PW25 under UV light was highest. The photocatalytic degradation by P25 seemed to enhance the appropriate elementary reactions to oxidize $C_2H_2$ into $CO_2$. On the other hand, it was inferred that BA-PW25 provided "weak active species" that are not so effective to oxidize organic species into $CO_2$ even if UV light was irradiated.

The opportunities for "weak active species" are lower potential holes formed or trapped by mid-gap levels located above the balance-band top. Since the byproduct formed on BA-PW25 by visible light irradiation was easily decomposed into $CO_2$ by UV irradiation, it is considered that the holes formed with the mid-gap levels and visible light may have lower oxidative powers than that with the valence-band top and UV light. However, these "weak active species" have slightly higher oxidative power than the "less active species" formed on N-$TiO_2$ with visible light, since the N-$TiO_2$ did not oxidize $C_2H_2$. The visible light absorption of N-$TiO_2$ is due to an electron excitation from an N-induced mid-gap level, which is isolated from the valence band [6,24,25] to the conduction band. This results in the formation of a hole on N-induced mid-gap level that is effective for the oxidation of acetaldehyde or 2-propanol [5,6] but not effective for the degradation of $C_2H_2$. From these considerations, it is inferred that the "weak active species" related to $C_2H_2$ degradation was a hole formed on the mid-gap level of BA-PW25 between the potentials of valence-band top of conventional $TiO_2$ and the N-induced mid-gap level of N-$TiO_2$ (Fig. 8). Based on the XRD and TG-DTA, the bulk of BA-PW25 was not oxygen-deficient. Therefore, the likely causes for the formation of mid-gap level may be due to manifold of surface state, such as oxygen defect, peroxide, and traces of sulfate and nitrate, formed by the impurities in the precursor of the photocatalyst. These issues are under consideration, and will be reported elsewhere.

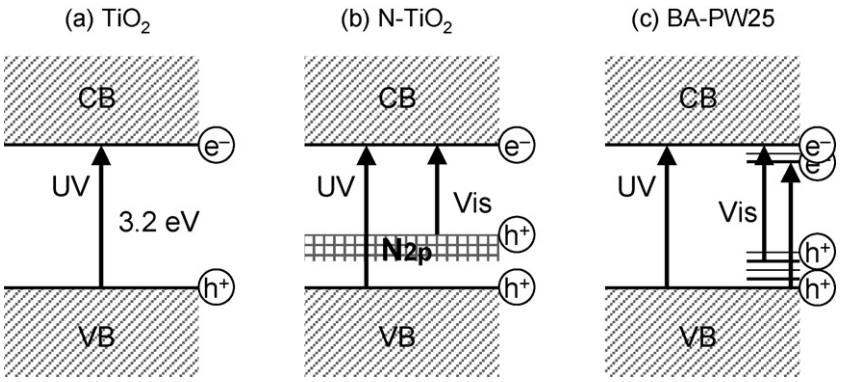


Fig. 8. Expected energy bands for BA-PW25 and N-$TiO_2$. VB and CB denote the valence and the conduction bands of the $TiO_2$ particles. Short solid lines represent mid-gap levels formed by surface manifold.

The dependence of $C_2H_2$ concentration on the photocatalytic removal rate of $C_2H_2$ was analyzed (Fig. 9(a)). The removal rates by BA-PW25 and P25 under UV light increased with increasing the $C_2H_2$ concentration in the range of 0–1000 ppm. This suggests that the removal rate depends on the amount of $C_2H_2$ adsorbed on the photocatalyst. Since the removal rate by BA-PW25 under UV light was ca. 60% of that observed with P25, we have to state that P25 utilizes UV light more efficiently than BA-PW25. On the other hand, under visible light, the removal rate of P25 was always zero, and BA-PW25 showed the higher efficiency. In these experiments, the UV-photon flux in UV light irradiation ($4.7 \times 10^{-9}$ mol cm$^{-2}$ s$^{-1}$) was smaller than the photon flux in visible-light irradiation ($8.0 \times 10^{-9}$ mol cm$^{-2}$ s$^{-1}$) in the wavelength range that can be absorbed by BA-PW25 ($400 < \lambda < 510$ nm). Therefore, the apparent quantum yields were in the order of P25 (UV) > BA-PW25 (UV) > BA-PW25 (Vis) > P25 (Vis).

Degradation of $C_2H_2$ were analyzed by assuming that the removal rate of $C_2H_2$ ($r$) is proportional to the amount of adsorbed $C_2H_2$ (Eq. (4)), which is expected from Langmuir's adsorption equation (Eq. (5)),

$$r = k\theta \tag{4}$$

$$\theta = \frac{Kc}{1 + Kc} \tag{5}$$

Table 1
Estimated values of rate constant ($k$) and adsorption constant ($K$) on the degradation of $C_2H_2$ by BA-PW25 and P25 photocatalyst under visible and UV light

| Sample | Light | $k$ (Pa h$^{-1}$) | $K$ (Pa$^{-1}$) |
|---|---|---|---|
| BA-PW25 | Vis | 0.011 | 0.034 |
| BA-PW25 | UV | 0.026 | 0.025 |
| P25 | UV | 0.027 | 0.075 |

$$\frac{1}{r} = \frac{1}{kK} \cdot \frac{1}{c} + \frac{1}{k} \tag{6}$$

where $k$, $K$, $c$, and $\theta$ denote rate constant, adsorption constant, $C_2H_2$ concentration, and occupation ratio, respectively. The plots of $1/r$ against $1/c$ (Eq. (6)) are roughly straight (Fig. 9(b)). The estimated $k$ and $K$ for BA-PW25 and P25 under visible and UV light were listed in Table 1. The adsorption constants ($K$) of BA-PW25 under UV and visible light were similar. This indicates that the effective number of adsorption sites is identical regardless of the wavelength irradiated. P25 showed the higher $K$ value than BA-PW25, suggesting that P25 possesses a larger number of adsorption site than BA-PW25, although the BET surface area of BA-PW25 (110 m$^2$ g$^{-1}$) was larger than that of P25 (50 m$^2$ g$^{-1}$). The reaction rate constants ($k$), of the two samples were not so different under UV light irradiation.

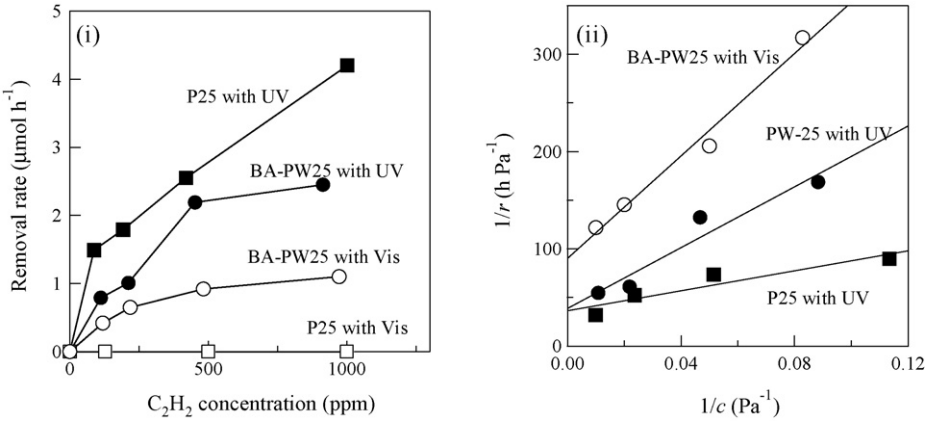


Fig. 9. (i) Dependence of $C_2H_2$ concentration ($c$) on initial degradation rate ($r$) and (ii) the plots of $1/r$ against $1/c$. (◯) BA-PW25 with visible light, (●) BA-PW25 with UV light, (□) P25 with visible light and (■) P25 with UV light.

However, the $k$ of BA-PW25 under visible light was significantly smaller than that under UV light. This is probably due to both the weak oxidative power of formed species on $C_2H_2$ degradation and the low absorption coefficient in the visible light region.

## 4. Conclusions

BA-PW25 photocatalyst, which was prepared by the calcination of titanium hydroxide precursor made from titanium (IV) sulfate and ammonia solution, was the only one that degraded $C_2H_2$ into $CO_2$ under visible light among the visible light responsive photocatalysts examined. The degradation rate under visible light was significantly smaller than that under UV light. Furthermore, BA-PW25 produced larger amounts of organic byproducts under both UV and visible light. It is considered that the amount of active species formed with visible light is small as compared with the conventional UV-initiated photocatalysis and that the active species are not effective to oxidize organic byproducts into $CO_2$. However, the active species (or hole) formed by BA-PW25 with visible light is stronger than that formed by N-$TiO_2$ prepared with gaseous $NH_3$ treatment of $TiO_2$.

The UV–vis absorption edge of BA-PW25 located at the longer wavelength than that of N-$TiO_2$, although XRD, XPS, and TG-DTA showed neither clear evidence for the presence of oxygen deficiency nor any special structures. Therefore, the relation between the novel degradation activity of BA-PW25 and the material structures is not clear at this stage. However, it is notable that BA-PW25 degrades $C_2H_2$ under visible light, since N-$TiO_2$, which is widely studied in this field, did not oxidize $C_2H_2$. It is inferred that the active species effective for $C_2H_2$ degradation were formed on the mid-gap level of BA-PW25 between the potentials of the valence-band top of conventional $TiO_2$ and the N-induced mid-gap level of N-$TiO_2$.

## Acknowledgements

This work was greatly supported by ECSAW program (Environmental Catalysis for Sustaining Clean Air and Water) in 2005–2006. We greatly appreciate Dr. J.M. Herrmann, Dr. M. Cattenot, and all the friends of Institut de recherches sur la catalyse et l'environnement de Lyon (IRCELYON), which was reorganized from Laboratoire d'Application de la Chimie a l'Environment (LACE) and l'Institut de Recherches sur la Catalyse (IRC) in 2007.

## References

[1] T. Ibusuki, K. Takeuchi, J. Mol. Catal. 88 (1994) 93.
[2] M.R. Hoffmann, S.T. Martin, W.Y. Choi, D.W. Bahnemann, Chem. Rev. 95 (1995) 69.
[3] T. Sano, N. Negishi, K. Takeuchi, S. Matsuzawa, Solar Energy 77 (2004) 543.
[4] S. Sato, Chem. Phys. Lett. 123 (1986) 126.
[5] R. Asahi, T. Morikawa, T. Ohwaki, K. Aoki, Y. Taga, Science 293 (2001) 269.
[6] H. Irie, Y. Watanabe, K. Hashimoto, J. Phys. Chem. B 107 (2003) 5483.
[7] S. Sato, R. Nakamura, S. Abe, Appl. Catal. A: Gen. 284 (2005) 131.
[8] M. Mrowetz, W. Balcerski, A.J. Colussi, M.R. Hoffman, J. Phys. Chem. B 108 (2004) 17269.
[9] T. Sano, N. Negishi, K. Koike, K. Takeuchi, S. Matsuzawa, J. Mater. Chem. 14 (2004) 380.
[10] T. Tachikawa, S. Tojo, K. Kawai, M. Endo, M. Fujitsuka, T. Ohno, K. Nishijima, Z. Miyamoto, T. Majima, J. Phys. Chem. B 108 (2004) 19299.
[11] H. Irie, Y. Watanabe, K. Hashimoto, Chem. Lett. 32 (2003) 772.
[12] T. Ohno, M. Akiyoshi, T. Umebayashi, K. Asai, T. Mitsui, M. Matsumura, Appl. Catal. A: Gen. 265 (2004) 115.
[13] K. Nukumizu, J. Nunoshige, T. Takata, J.N. Kondo, M. Hara, H. Kobayashi, K. Domen, Chem. Lett. 32 (2003) 196.
[14] I. Nakamura, N. Negishi, S. Kutsuna, T. Ihara, S. Sugihara, E. Takeuchi, J. Mol. Catal. A: Chem. 161 (2000) 205.
[15] T. Ihara, M. Miyoshi, Y. Iriyama, O. Matsumoto, S. Sugihara, Appl. Catal. B: Environ. 42 (2003) 403.
[16] Sugihara, Zukai Hikarishokubai-no subete, Kogyo Chousakai, Tokyo, 2003, p. 122.
[17] F. Thevenet, O. Guaitella, J.M. Herrmann, A. Rousseau, C. Guillard, Appl. Catal. B: Environ. 61 (2005) 58.
[18] B.J. Finlayson-Pitts, J.N. Pitts Jr., Atmospheric Chemistry, Wiley-Interscience, New York, 1986.
[19] F. Izumi, T. Ikeda, Mater. Sci. Forum 321–324 (2000) 198.
[20] H.M. Yates, M.G. Nolan, D.W. Sheel, M.E. Pemble, J. Photochem. Photobiol. A: Chem. 179 (2006) 213.
[21] O. Diwald, T.L. Thompson, T. Zubkov, E.G. Goralski, S.D. Walck, J.T. Yates, J. Phys. Chem. B 108 (2004) 6004.
[22] Z.S. Lin, A. Orlov, R.M. Lambert, M.C. Payne, J. Phys. Chem. B 109 (2005) 20948.
[23] A. Rousseau, O. Guaitella, L. Gatilova, F. Thevenet, C. Guillard, J. Ropcke, G.D. Stancu, Appl. Phys. Lett. 87 (2005) 221501.
[24] R. Nakamura, T. Tanaka, Y. Nakato, J. Phys. Chem. B 108 (2004) 10617.
[25] S. Sakthivel, H. Kisch, Chemphyschem 4 (2003) 87.